



OPEN Placental MRI texture features in prenatal exposure to opioids and tobacco

Jonathan A. Class^{1,6}, Ramana V. Vishnubhotla^{1,6}, David M. Haas², Ilana W. Hull³, Senthilkumar Sadhasivam⁴ & Rupa Radhakrishnan^{1,5}✉

Opioid use disorder during pregnancy significantly increases the likelihood of adverse developmental outcomes in the offspring. Texture analysis serves as a quantitative technique that could be vital in identifying microstructural variations in placentas that have been exposed to opioids and other substances. This is a prospective, multisite cross-sectional study that recruited pregnant women that were greater than 16 weeks of gestation. We manually segmented placenta tissue from half-Fourier single-shot turbo spin-echo (HASTE) sequence MR images. We then assessed placental surface area and texture features using a radiomics pipeline. Using linear models, we assessed the association of substance use on placental surface area and texture features, accounting for demographic characteristics. There were 33 pregnant women with opioid use and 29 controls. Based on regression analysis, opioid exposure was associated with alterations in two texture features while tobacco exposure was associated with alterations in five texture features prior to multiple comparison correction. These were no longer significant after correcting for multiple comparisons. Additionally, tobacco exposure was significantly associated with greater placenta surface area.

Keywords Placenta MRI, Placenta texture, Radiomics, Fetal MRI, Prenatal opioid exposure, Prenatal tobacco exposure

Abbreviations

2D	Two-dimensional
3D	Three-dimensional
AIDS	Acquired immunodeficiency syndrome
CTB	Cytotrophoblast
FDR	False discovery rate
GLCM	Gray level co-occurrence matrix
GLDZM	Gray level distance zone matrix
GLRLM	Gray level run length matrix
GLSZM	Gray level size zone matrix
HASTE	Half-Fourier single-shot turbo spin-echo
HIV	Human immunodeficiency virus
IRB	Institutional Review Board
MRI	Magnetic resonance imaging
NGLDM	Neighborhood gray level dependence matrix
NGTDM	Neighborhood gray tone dependence matrix
POE	Prenatal opioid exposure
TE	Echo time
TR	Repetition time
VIF	Variance inflation factor

¹Department of Radiology and Imaging Sciences, Indiana University School of Medicine, Indianapolis, IN, USA. ²Department of Obstetrics and Gynecology, Indiana University School of Medicine, Indianapolis, IN, USA. ³Department of Medicine, University of Pittsburgh Medical Center, Pittsburgh, PA, USA. ⁴Department of Anesthesiology & Perioperative Medicine, University of Pittsburgh Medical Center, Pittsburgh, PA, USA. ⁵Indiana University School of Medicine, 705 Riley Hospital Drive, Indianapolis, IN 46202, United States of America. ⁶Jonathan A. Class and Ramana V. Vishnubhotla contributed equally to this work. ✉email: rradhak@iu.edu

Substance use disorder affects a significant number of pregnant women in the U.S. From a 2019 survey, 6.6% of women reported opioid use during pregnancy. Of these women, 21.2% reported misuse, 27.1% indicated a desire to reduce usage, and 31.9% did not receive proper guidance in the impact of opioid use on the infant¹. Additionally, smoking rates of pregnant women with opioid use disorder has been estimated at 88%². Substance use disorder during pregnancy has been associated with maternal and fetal morbidity and mortality. Existing studies show prenatal opioid exposure to be associated with poor fetal development^{3,4}. The placenta is a vital physiological link between opioid exposure in pregnant women and fetal developmental impacts. However, the impact of substance use disorder on the placenta and its impact on placental structure and function are still poorly understood.

The placenta plays an important role in fetal development and neuroprotection. Its functions range from nutrition and gas exchange to involvement in the endocrine and immune systems⁵. The placenta also produces neurotransmitters that may affect fetal brain development⁶ and associations of placental changes to infant neurobehavior suggests the presence of a placenta-brain axis⁷⁻⁹. Appropriate placental development is essential to fetal and maternal health with placental dysfunction leading to a myriad of adverse outcomes including fetal growth restriction, preterm birth, and preeclampsia¹⁰.

Although the impacts of prenatal substance exposure on the developing placenta are in general understudied, most literature is based on preclinical or retrospective ex-vivo data from human studies. Data from ex-vivo studies have shown associations between substance use in pregnancy and adverse placental structure and function including poor placental vascularization and perfusion and inadequate nutrient transport^{11,12}. An ex vivo birth cohort study revealed increased placental weight and placental weight/birth weight ratio among smokers compared to nonsmokers¹³, likely due to placental villous alterations in the setting of tobacco use^{14,15}. Similarly, a small cohort retrospective study in prenatal opioid exposure showed delayed placental villous maturation and placentomegaly¹⁶.

Given the complexity of the placental anatomy throughout gestation, assessing in vivo placental development is key to understanding early effects of substance exposure on the placenta, and impacts of early interventions. Both ultrasound and MRI have been used in clinical assessment of the placenta in vivo in healthy and high-risk pregnancies, and those with placenta fetal pathology¹⁷. Apart from linear measurements of placental size, these assessments are typically based on qualitative and visual evaluation of placental features, and are subject to observer variability that may limit their clinical use¹⁸. Recent studies have investigated the use of automated quantitative methods to stage placental maturity with ultrasound¹⁹ and MRI²⁰⁻²³ and hold great promise in objective and standardized assessments of placental development that may lead to more personalized medical management. Specifically, placental texture analysis has shown gestational age dependent maturational changes in the placenta in healthy pregnancies²¹, that are altered in disease states such as placenta accreta and fetal growth restriction²⁴⁻²⁷. Given the histological changes that are present in the placenta in maternal substance exposure, and their potential impacts on future neurodevelopment in the offspring, noninvasive quantitative assessment of the placenta in vivo is a crucial tool in management decisions. Our team has previously reported on larger placental volumes in pregnant women with prenatal opioid exposure and concomitant tobacco use²⁸, and in this proposed study, we will build upon our prior work to specifically assess microstructural alterations in the placenta through placental texture alterations on placental MRI in a prospectively recruited cohort of pregnant women using opioids.

Results

Demographic and clinical data

There were 80 subjects with MR images of the placenta available for review. There were 18 subjects who were excluded due to poor image quality. Demographic information for these excluded subjects can be found in Supplemental Table 1. Finally, 62 subjects were included in the analysis – 33 in the prenatal opioid exposure (POE) group and 29 control subjects. Twenty subjects had at least one slice excluded for texture analysis. Two subjects had more than 25% of their volume excluded. Since our texture analysis was done using 2D slices, excluded slices did not affect second order texture analysis calculations. 58 subjects (93.5%) had axial, sagittal, and coronal images available for review. The sagittal plane was used to segment the placenta in 41 subjects. Twenty five subjects (75.8%) in the POE group also smoked tobacco. No control subjects smoked tobacco. Demographic information is shown in Table 1.

Dice similarity coefficient

Intra-rater reliability was assessed by calculating the average of the Dice similarity coefficient. Ten (16%) of the placentas were re-segmented at least three weeks after the original segmentation by the same individual. The Dice coefficient was calculated by comparing these two segmentations of the same placenta at different time points. The average of the Dice similarity coefficient was 0.9043 with a standard deviation of 0.034, indicating a high degree of similarity between the two segmentations.

Collinearity of substance exposure

Since 76% of those with opioid use also had tobacco use, we tested the collinearity between these two variables. The Pearson's correlation coefficient was 0.77, the tolerance based on correlation is 0.41, and the variance inflation factor (VIF) was 2.46. All these metrics suggest moderate collinearity.

Association of opioid exposure to texture features

Two second order texture features were associated with maternal opioid use (Table 2). Greater small zone low gray level emphasis and low dependence low gray level emphasis were associated with opioid exposure prior to multiple comparison correction. Both metrics assess the quantification of low gray levels in an image.

	Opioid	Control	<i>p</i> -value
Number	33	29	
Fetal sex - male	18 (55%)	8 (28%)	0.04*†
Maternal age in years (SD)	30.2 (4.5)	29 (4.4)	0.30‡
Gestational age in weeks (SD)	33.6 (4.3)	31.8 (4.1)	0.10‡
Tobacco exposure	25 (76%)	0 (0%)	<0.01*†
Location - IU	24 (73%)	21 (72%)	1.00†
Race			<0.01*†
White	25 (76%)	17 (59%)	
Black/African American	1 (3%)	9 (31%)	
White/Hispanic	1 (3%)	2 (7%)	
Mixed	6 (18%)	1 (3%)	
Body mass index	33.4 (6.1)	34.7 (5.5)	0.38‡
Hypertension	5 (15%)	1 (3%)	0.20†

Table 1. Demographic and clinical Information. *Denotes significant difference between the groups. † Fisher's exact test. ‡ Independent t-test.

	Category	t-stat	<i>p</i> -value	FDR
Small zone low gray level emphasis	GLSZM	2.26	0.031	0.495
Low dependence low gray level emphasis	NGLDM	2.27	0.031	0.262

Table 2. Association of texture features with opioid exposure. Texture features which were significantly associated with opioid exposure for individual comparisons ($p < 0.05$) based on a linear regression. Significance was not maintained after multiple comparison correction for false discovery rate (FDR).

	Category	t-stat	<i>p</i> -value	FDR
Normalized inverse difference moment	GLCM	-2.01	0.050	0.521
Zone size non-uniformity	GLSZM	2.05	0.048	0.351
Zone distance non-uniformity	GLDZM	2.43	0.021	0.273
Dependence non-uniformity	NGLDM	2.07	0.046	0.280
Coarseness	NGTDM	2.08	0.043	0.214

Table 3. Association of texture features with tobacco exposure. Texture features which were significantly associated with tobacco exposure for individual comparisons ($p < 0.05$) based on a linear regression. Significance was not maintained after multiple comparison correction for false discovery rate (FDR).

Association of tobacco exposure to texture features

Five second order texture features were significantly associated with maternal smoking. Significant texture features are depicted in Table 3. Lower normalized inverse difference moment, a measure of homogeneity, was associated with tobacco exposure. Greater zone size non-uniformity (GLSZM), zone distance non-uniformity (GLDZM), and dependence non-uniformity (NGLDM) were all also associated with tobacco exposure. Non-uniformity assesses the similarity/variability of a characteristic (zone size, zone distance, or dependence) within an image, with a greater value indicating lower homogeneity. Finally, more coarseness (NGTDM) was also associated with tobacco exposure. None of the GLRLM features showed significant associations.

Association of substance exposure to surface mesh area

Using linear models, the impact of substance exposure on placenta surface area were assessed. Tobacco exposure ($t = 2.68$; $p = 0.01$), but not opioid exposure ($t = -1.84$; $p = 0.07$), was significantly linked to greater placental surface area.

Association of fetal sex and gestational age to texture and surface area

Fetal sex was not associated with any differences in texture features or surface area after multiple comparison correction. Gestational age, however, was associated with lower contrast ($t = 3.05$, $p = 0.005$) and increased placenta surface area ($t = 6.32$, $p < 0.001$).

Discussion

Summary of results

In this study, we identified that opioid use and tobacco use in pregnant women were associated with altered placenta texture features on individual assessments, but not when corrected for multiple comparisons. We also identified tobacco exposure to significantly associated with greater placental surface area after accounting for multiple comparison correction.

The two texture features that were positively associated with maternal opioid use on individual comparisons were small zone low gray level emphasis (GLSZM) and low dependence low gray level emphasis (NGLDM). Both these features assess the quantification and distribution of low gray levels which corresponds to a greater number of smaller, darker regions associated with opioid exposure. Five texture features that were significantly associated with tobacco exposure included one feature each for GLCM, GLSZM, GLDZM, NGLDM, and NGTDM. Greater zone size non-uniformity (GLSZM), zone distance non-uniformity (GLDZM), and dependence non-uniformity (NGLDM) are all measures of non-uniformity, indicating that tobacco exposure was associated with greater placental heterogeneity. The NGTDM feature, coarseness, that was significantly associated with tobacco exposure, can be contrasted with busyness. A coarser image has varying levels of gray tone but with more gradual changes; whereas, busyness would be smaller areas of greater change in intensity²⁹. While these changes in radiomic features could potentially correspond to placental vascular and microstructural alterations, this is yet to be investigated. Since significant texture features did not survive multiple comparison correction, it is important to note that our findings may be considered exploratory.

Comparison to literature

Previous literature has shown placental MRI texture features to be associated with gestational age and fetal sex. One study found a positive correlation with several Haralick (GLCM) texture features corresponding to heterogeneity and gestational age;³⁰ another study found gray level run length matrix (GLRLM) significant with gestational age²⁶. Additionally, the latter study found texture differences between healthy male and female fetuses suggesting greater homogeneity and symmetry in male fetuses²⁴. Our study did not have any association between fetal sex and texture features. Additionally, only one texture feature, contrast, was significantly associated with gestational age.

Implications

This is the first study to show greater in-vivo placental surface area associated with tobacco use. Previous studies showed greater placental weight to birth weight ratio after delivery¹³ and greater placental volume in-vivo²⁸ associated with prenatal tobacco exposure. Considering that tobacco exposure was associated with increased placenta size and possibly increased texture heterogeneity suggest that it may facilitate placenta maturation. MRI texture metrics may be related to maturing cotyledons (Fig. 1), the functional unit of the placenta involved with the exchange of oxygen and other nutrients. Since increased heterogeneity has been linked to increased gestational age,³⁰ this would suggest that based on texture analysis, these placentas may show signs of increased maturation. This would be in line with previous results where smoking was linked with increased maturation of the placenta³⁰.

While tobacco smoking may be linked to larger and possibly more mature placentas, it may not indicate that growth and maturation is healthy. Maternal smoking is shown to impact the balance between proliferation and differentiation in cytotrophoblasts (CTBs)³¹, possibly by increased fetal hypoxia³² and upregulated CTB expression of von Hippel-Lindau tumor-suppressor protein³³. This alteration of the balance between proliferation and differentiation of CTBs due to hypoxia and nicotine exposure may explain the increased placenta growth associated with tobacco exposure. Even if CTB differentiation is greater in the presence of tobacco exposure, it is unknown if this is due to natural maturation or if the natural tissue composition is altered or pathological. Without further analysis based on tissue specimens, the association of texture features and tissue composition remains unclear.

Strengths and limitations

One strength of our study is our reasonable sample size. It can be challenging to recruit pregnant women with substance exposure, so having 80 placentas to review was an advantage. Another strength of our study is its prospective nature, which allows us to limit bias and confounders to some degree. High intra-rater Dice similarity coefficient indicates high reproducibility when segmented by a single researcher. Conceptually, in-vivo texture analysis is a unique way of understanding tissue composition.

We also have limitations to mention. Multisite MRI can introduce variability when using radiomics as signal intensities are not based on physical properties. However, the two recruitment sites used the same acquisition parameters with intensity normalization prior to texture analysis and scanner site was included as a covariate.

Given no controls were exposed to tobacco, it may be challenging to isolate the impact of tobacco alone. However, our results remain representative of mothers with prenatal opioid exposure given the high percentage of polysubstance exposure, specifically tobacco, in this population. Rates of tobacco smoking in this population have been reported at 88%² with our sample being at 75.8%. There was moderate collinearity between opioid and tobacco use (VIF = 2.46), which could be a potential cause for overlapping influence.

Finally, our control group had a significantly higher proportion of Black/African American subjects. This may be an important consideration as race has previously been linked to differences in placenta characteristics^{34,35}. We accounted for the effect of race by using it as a co-variate in our linear model. Overall, the results of our study suggest the possibility of some association with tobacco and opioid co-exposure using a novel and promising analytical method of in-vivo assessment of placental health.

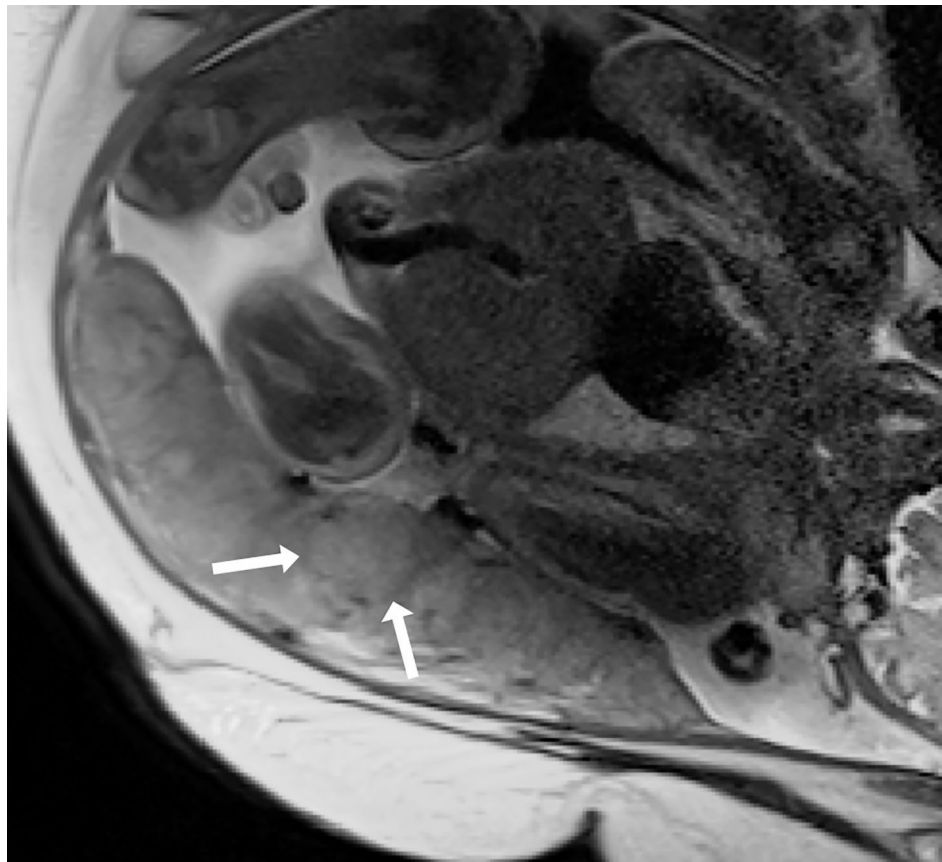


Fig. 1. Half-Fourier Single-shot Turbo spin-Echo (HASTE) through the placenta showing the placental cotyledon surrounded by connective tissue, septa, seen as hypointense lines (arrow).

Conclusions

Using radiomic pipelines to calculate texture features could be a promising method to structurally assess placenta health which go beyond the capabilities of visual human assessment. This study presents some noteworthy findings where texture analysis was used to assess the impact prenatal substance exposure on placenta growth and maturation. The findings suggest that tobacco exposure is associated with greater placental surface area and may also impact placental maturation.

Methods

Subjects

This is a prospective, IRB approved, multisite cross-sectional study that recruited pregnant women that were greater than 16 weeks of gestation. The sites for this study were Indiana University School of Medicine and the University of Pittsburgh Medical Center. Informed consent was obtained and the study was conducted in accordance with the Declaration of Helsinki³⁶. The Institutional Review Board of Indiana University was the primary IRB that approved the project, with a Reliance agreement with the University of Pittsburgh IRB. There were two groups – women exposed to opioids during pregnancy and control pregnant women who were not exposed to opioids. All the women with prenatal opioid exposure were on medication for opioid use disorder (MOUD) with either buprenorphine or methadone. Hypertension was defined as maternal chronic hypertension or preeclampsia/eclampsia for current pregnancy. Exclusion criteria included MRI contraindications, serious maternal medical illness, HIV/AIDS, and major fetal congenital abnormalities. Demographic information and clinical data were obtained by patient interview and electronically stored on REDCap^{37,38} hosted at Indiana University School of Medicine.

MRI acquisition

Fetal-placental MRI was performed in the second or third trimester. All women at the Indiana University site underwent the same imaging protocol on a 3 T Siemens Skyra or 3 T Siemens Vida Fit scanner (Erlangen, Germany) with a 16-channel body coil. The University of Pittsburgh site underwent the same imaging protocol on a 3 T Siemens Skyra scanner. Two-dimensional (2D) MR images of the placenta were acquired using a Half-Fourier Single-shot Turbo spin-Echo (HASTE) sequence in the sagittal, axial, and coronal for most subjects. Acquisition parameters for both sites were: TE = 78.00 ms, TR = 1110 ms, resolution = 256 × 230, 42 slices, 3 mm slice thickness, and total acquisition time of 48 s. No sedation or contrast was used.

Placenta MRI segmentation

Placenta region of interest masks were manually segmented by a single researcher using ITK-Snap (Fig. 2)³⁹. Placenta segmentation quality was reviewed with a pediatric radiologist. Given motion artifact is given in fetal imaging, the highest quality plane was chosen for segmentation with the sagittal image preferred as it gave the clearest delineation of the placental and myometrial interface. Subjects were excluded when frank signal drop and artifact affected over 50% of the placental volume. Subjects with slices that contained artifact had those slices excluded in the texture analysis but included in the volume analysis as integrity of placental border could be assessed. The average of the Dice Similarity Coefficient^{40,41} was calculated for a sample of the subjects to assess the intra-rater reliability. As there was only one researcher performing the segmentations, inter-rater reliability was not assessed.

Texture analysis

Placenta MR images along with corresponding segmented masks were run through a radiomics pipeline within MATLAB^{42,43}. MR images were normalized, and mask images were slightly eroded along the edges prior to performing texture analysis. The fixed bin number was 200. Second order texture features based on gray level co-occurrence matrix (GLCM, 25 texture features) and gray level run length matrix (GLRLM, 16 texture features) were chosen as these have previously been assessed in fetal studies^{24,26}.

Additional second order texture features assessed were gray level size zone matrix (GLSZM, 16 texture features), gray level distance zone matrix (GLDZM, 16 texture features), neighborhood gray tone difference matrix (NGTDM, 5 texture features), and neighborhood gray level dependence matrix (NGLDM, 16 texture features). Texture features were quantified based on an average of 2D resampled slices.

Second order texture feature categories

Second order texture analysis quantifies the spatial relationship of varying gray tones in an image using matrices. In the case of MRI analysis, the different gray tones represent the different signal intensities of pixels (2D slice) or voxels (3D). Each texture category has a different method of transforming the varied intensity arrangement into a matrix and each has different equations, features, for these matrices to quantify this information.

Gray level co-occurrence matrix (GLCM) uses pairs of pixels at a defined distance and direction to construct a matrix⁴⁴. Fig. 3 demonstrates a matrix with distance and direction one pixel to the right. Gray level run length matrix (GLRLM) and gray level size zone matrix (GLSZM) follow similar techniques as GLCM though they look at runs of identical intensities and groups of identical intensities respectively⁴⁵. Gray level zone distance matrix (GLZDM) is a subset of GLSZM⁴⁶. Neighborhood gray tone difference matrix (NGTDM) and neighborhood grey level dependence matrix (NGLDM) compare the intensity of a pixel with the average intensity values of its neighboring pixels with various criteria^{29,47,48}.

Placental surface area measurements

Placental surface area was calculated using a radiomics pipeline within MATLAB^{42,43}. MR images were normalized, and shape characteristics were calculated for surface mesh area. Surface area was quantified based on resampled 3D data.

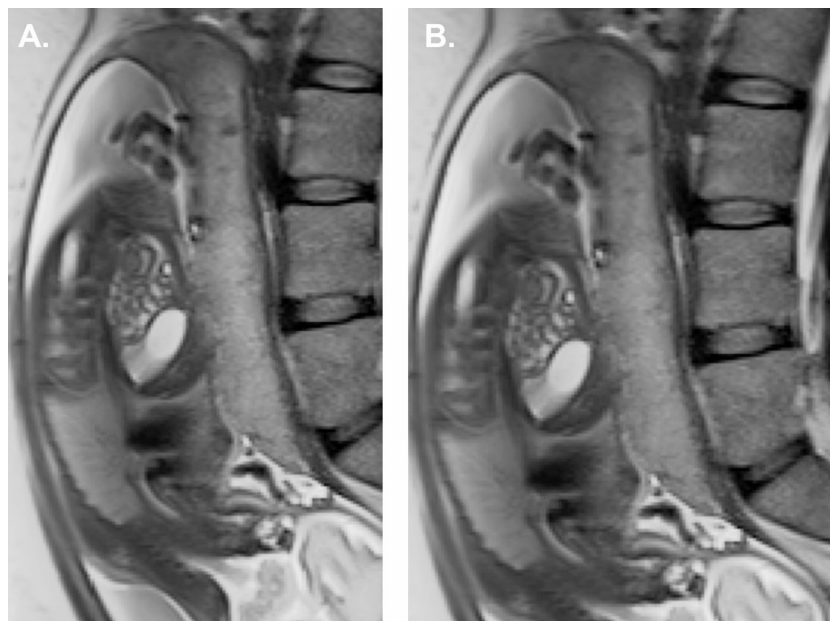


Fig. 2. (a) Half-Fourier Single-shot Turbo spin-Echo (HASTE) sequence MRI slice of a fetus in the sagittal plane and (b) the placenta segmented in red.

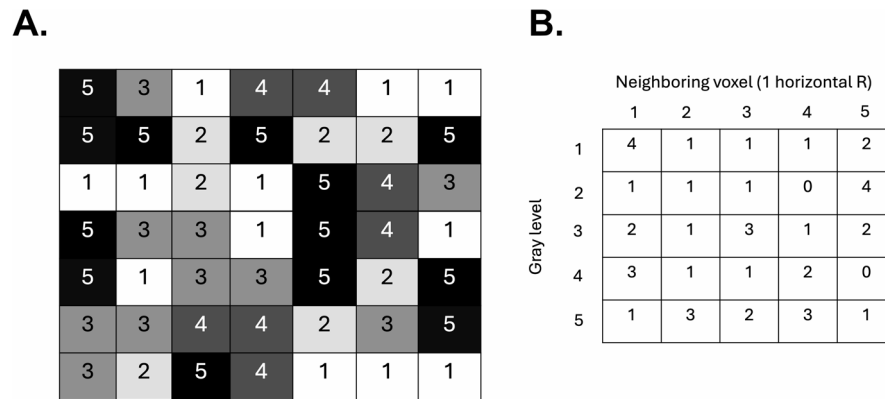


Fig. 3. An example of a ROI **a)** with varied gray tones and **b)** its corresponding gray level cooccurrence matrix (GLCM). Distance and direction are neighboring pixel to the right.

Statistical analysis

Significance for demographic data was calculated either with an independent t-test assuming unequal variances for numerical variables or a Fisher's exact test for categorical variables. For radiomic data, a multivariable linear regression was performed to assess the impact of prenatal exposure to opioids and tobacco on placenta texture features, volume, and surface area. Demographic variables including fetal sex, race, gestational age, maternal body mass index (BMI), hypertension, and scanner site were used as covariates. Placenta volume was also included in the analysis. The threshold for significance for individual comparisons was a p-value < 0.05. Multiple comparison correction was also performed using the Benjamini-Hochberg procedure⁴⁹, which is considered the false discovery rate (FDR). P-value of < 0.05 was considered significant for FDR. Multicollinearity was also calculated for demographic variables based on Pearson's correlation coefficient, tolerance, and variance inflation factor.

Data availability

Data can be made available upon request to the corresponding author.

Received: 28 August 2025; Accepted: 4 November 2025

Published online: 15 December 2025

References

- Ko, J. Y. et al. Vital Signs: Prescription Opioid Pain Reliever Use During Pregnancy – 34 U.S. Jurisdictions, 2019. *MMWR Morb Mortal Wkly Rep* <https://doi.org/10.15585/mmwr.mm6928a1> **69**, 897–903 (2020).
- Jones, H. E. et al. Smoking in pregnant women screened for an opioid agonist medication study compared to related pregnant and non-pregnant patient samples. *Am. J. Drug Alcohol Abuse*. **35**, 375–380. <https://doi.org/10.1080/00952990903125235> (2009).
- Graeve, R. et al. Infants' prenatal exposure to opioids and the association with birth outcomes: A systematic review and meta-analysis. *Paediatr. Perinat. Epidemiol.* **36**, 125–143. <https://doi.org/10.1111/ppe.12805> (2022).
- Radhakrishnan, R. et al. Pilot study of fetal brain development and morphometry in prenatal opioid exposure and smoking on fetal MRI. *J. Neuroradiol.* **49**, 53–58. <https://doi.org/10.1016/j.neurad.2020.12.004> (2022).
- Stern, C. et al. Placental endocrine activity: adaptation and disruption of maternal glucose metabolism in pregnancy and the influence of fetal sex. *Int. J. Mol. Sci.* **22** <https://doi.org/10.3390/ijms222312722> (2021).
- Rosenfeld, C. S. The placenta-brain-axis. *J. Neurosci. Res.* **99**, 271–283. <https://doi.org/10.1002/jnr.24603> (2021).
- Green, B. B. et al. Expression of imprinted genes in placenta is associated with infant neurobehavioral development. *Epigenetics* **10**, 834–841. <https://doi.org/10.1080/15592294.2015.1073880> (2015).
- Lesseur, C. et al. Sex-specific associations between placental leptin promoter DNA methylation and infant neurobehavior. *Psychoneuroendocrinology* **40**, 1–9. <https://doi.org/10.1016/j.psyneuen.2013.10.012> (2014).
- Marsit, C. J. et al. Placenta-imprinted gene expression association of infant neurobehavior. *J. Pediatr* **160**, 854–860 e852 <https://doi.org/10.1016/j.jpeds.2011.10.028> (2012).
- Wardinger, J. E. & Ambati, S. in *StatPearls* (2024).
- Miller, C. B. & Wright, T. Investigating mechanisms of stillbirth in the setting of prenatal substance use. *Acad. Forensic Pathol.* **8**, 865–873. <https://doi.org/10.1177/1925362118821471> (2018).
- Ortigosa, S. et al. Feto-placental morphological effects of prenatal exposure to drugs of abuse. *Reprod. Toxicol.* **34**, 73–79. <https://doi.org/10.1016/j.reprotox.2012.04.002> (2012).
- Mitsuda, N. et al. Association between maternal active smoking during pregnancy and placental weight: the Japan environment and children's study. *Placenta* **94**, 48–53. <https://doi.org/10.1016/j.placenta.2020.04.001> (2020).
- Mayhew, T. M. Patterns of villous and intervillous space growth in human placentas from normal and abnormal pregnancies. *Eur. J. Obstet. Gynecol. Reprod. Biol.* **68**, 75–82. [https://doi.org/10.1016/0301-2115\(96\)02486-4](https://doi.org/10.1016/0301-2115(96)02486-4) (1996).
- Bush, P. G. et al. A quantitative study on the effects of maternal smoking on placental morphology and cadmium concentration. *Placenta* **21**, 247–256. <https://doi.org/10.1053/plac.1999.0470> (2000).
- Staszewski, C. et al. Histological Changes Observed in Placentas Exposed to Medication-Assisted Treatment. *J. Pregnancy* **2021**, 2175026 <https://doi.org/10.1155/2021/2175026> (2021).
- Hills, D., Irwin, G. A., Tuck, S. & Baim, R. Distribution of placental grade in high-risk gravidas. *AJR Am. J. Roentgenol.* **143**, 1011–1013. <https://doi.org/10.2214/ajr.143.5.1011> (1984).
- Fadl, S., Moshiri, M., Fligner, C. L., Katz, D. S. & Dighe, M. Placental imaging: normal appearance with review of pathologic findings. *Radiographics* **37**, 979–998. <https://doi.org/10.1148/rg.2017160155> (2017).

19. Lei, B. et al. Discriminative learning for automatic staging of placental maturity via Multi-layer fisher vector. *Sci. Rep.* **5**, 12818. <https://doi.org/10.1038/srep12818> (2015).
20. Abaci Turk, E. et al. Placental MRI: developing accurate quantitative measures of oxygenation. *Top. Magn. Reson. Imaging.* **28**, 285–297. <https://doi.org/10.1097/rmr.0000000000000221> (2019).
21. Andescavage, N. et al. Normative placental structure in pregnancy using quantitative magnetic resonance imaging. *Placenta* **112**, 172–179. <https://doi.org/10.1016/j.placenta.2021.07.296> (2021).
22. Aviles Verderra, J. et al. Real-time fetal brain and placental T2* mapping at 0.55T MRI. *Magn. Reson. Med.* **94**, 615–624. <https://doi.org/10.1002/mrm.30497> (2025).
23. León, R. L. et al. Intravoxel incoherent motion MR imaging analysis for diagnosis of placenta accreta spectrum disorders: A pilot feasibility study. *Magn. Reson. Imaging.* **80**, 26–32. <https://doi.org/10.1016/j.mri.2021.03.007> (2021).
24. Dahdouh, S. et al. In vivo placental MRI shape and textural features predict fetal growth restriction and postnatal outcome. *J. Magn. Reson. Imaging.* **47**, 449–458. <https://doi.org/10.1002/jmri.25806> (2018).
25. Do, Q. N. et al. Texture analysis of magnetic resonance images of the human placenta throughout gestation: A feasibility study. *PLoS One.* **14**, e0211060. <https://doi.org/10.1371/journal.pone.0211060> (2019).
26. Andescavage, N. et al. In vivo textural and morphometric analysis of placental development in healthy & growth-restricted pregnancies using magnetic resonance imaging. *Pediatr. Res.* **85**, 974–981. <https://doi.org/10.1038/s41390-019-0311-1> (2019).
27. Romeo, V. et al. Machine learning analysis of MRI-derived texture features to predict placenta accreta spectrum in patients with placenta previa. *Magn. Reson. Imaging.* **64**, 71–76. <https://doi.org/10.1016/j.mri.2019.05.017> (2019).
28. Wise, R. L. et al. Placental volume in pregnant women with opioid use: prenatal MRI assessment. *J. Matern Fetal Neonatal Med.* **36**, 157256. <https://doi.org/10.1080/14767058.2022.2157256> (2023).
29. Amadasun, M. & King, R. Textural features corresponding to textural properties. *IEEE Trans. Syst. Man. Cybernetics.* **19**, 1264–1274. <https://doi.org/10.1109/21.44046> (1989).
30. Pinette, M. G., Loftus-Brault, K., Nardi, D. A. & Rodis, J. F. Maternal smoking and accelerated placental maturation. *Obstet. Gynecol.* **73**, 379–382 (1989).
31. Zdravkovic, T., Genbacev, O., McMaster, M. T. & Fisher, S. J. The adverse effects of maternal smoking on the human placenta: a review. *Placenta* **26 Suppl A**, 81–86. <https://doi.org/10.1016/j.placenta.2005.02.003> (2005).
32. Socol, M. L., Manning, F. A., Murata, Y. & Druzin, M. L. Maternal smoking causes fetal hypoxia: experimental evidence. *Am. J. Obstet. Gynecol.* **142**, 214–218. [https://doi.org/10.1016/s0002-9378\(16\)32339-0](https://doi.org/10.1016/s0002-9378(16)32339-0) (1982).
33. Genbacev, O., Krtolica, A., Kaelin, W. & Fisher, S. J. Human cytotrophoblast expression of the von Hippel-Lindau protein is downregulated during uterine invasion in situ and upregulated by hypoxia in vitro. *Dev. Biol.* **233**, 526–536. <https://doi.org/10.1006/dbio.2001.0231> (2001).
34. Matoba, N. et al. Racial differences in placental pathology among very preterm births. *Placenta* **83**, 37–42. <https://doi.org/10.1016/j.placenta.2019.06.385> (2019).
35. Sletner, L. et al. Placental weight, surface area, shape and thickness - Relations with maternal ethnicity and cardio-metabolic factors during pregnancy. *Placenta* **148**, 69–76. <https://doi.org/10.1016/j.placenta.2024.02.002> (2024).
36. World Medical, A. World medical association declaration of helsinki: ethical principles for medical research involving human subjects. *JAMA* **310**, 2191–2194. <https://doi.org/10.1001/jama.2013.281053> (2013).
37. Harris, P. A. et al. Research electronic data capture (REDCap)—a metadata-driven methodology and workflow process for providing translational research informatics support. *J. Biomed. Inf.* **42**, 377–381. <https://doi.org/10.1016/j.jbi.2008.08.010> (2009).
38. Harris, P. A. et al. The REDCap consortium: Building an international community of software platform partners. *J. Biomed. Inf.* **95**, 103208. <https://doi.org/10.1016/j.jbi.2019.103208> (2019).
39. Yushkevich, P. A., Yang, G. & Gerig, G. ITK-SNAP: an interactive tool for semi-automatic segmentation of multi-modality biomedical images. *Annu. Int. Conf. IEEE Eng. Med. Biol. Soc.* **2016**, 3342–3345. <https://doi.org/10.1109/EMBC.2016.7591443> (2016).
40. Dice, L. R. Measures of the amount of Ecologic association between species. *Ecology* **26**, 297–302. <https://doi.org/10.2307/1932409> (1945).
41. Zou, K. H., Wells, W. M., Kikinis, R., Warfield, S. K. & rd, & Three validation metrics for automated probabilistic image segmentation of brain tumours. *Stat. Med.* **23**, 1259–1282. <https://doi.org/10.1002/sim.1723> (2004).
42. Vallieres, M., Freeman, C. R. & Skamene, S. R. El Naqa, I. A radiomics model from joint FDG-PET and MRI texture features for the prediction of lung metastases in soft-tissue sarcomas of the extremities. *Phys. Med. Biol.* **60**, 5471–5496. <https://doi.org/10.1088/0031-9155/60/14/5471> (2015).
43. Clark, K. et al. The cancer imaging archive (TCIA): maintaining and operating a public information repository. *J. Digit. Imaging.* **26**, 1045–1057. <https://doi.org/10.1007/s10278-013-9622-7> (2013).
44. Haralick, R. M., Shanmugam, K. & Dinstein, I. Textural features for image classification. *IEEE Trans. Syst. Man. Cybernetics.* **SMC-3**, 610–621. <https://doi.org/10.1109/TSMC.1973.4309314> (1973).
45. Galloway, M. M. Texture analysis using Gray level run lengths. *Comput. Graphics Image Process.* **4**, 172–179. [https://doi.org/10.1016/00146-664X\(75\)80008-6](https://doi.org/10.1016/00146-664X(75)80008-6) (1975). <https://doi.org/https://>
46. Thibault, G., Angulo, J. & Meyer, F. Advanced statistical matrices for texture characterization: application to cell classification. *IEEE Trans. Biomed. Eng.* **61**, 630–637. <https://doi.org/10.1109/TBME.2013.2284600> (2014).
47. Sun, C. & Wee, W. G. Neighboring Gray level dependence matrix for texture classification. *Comput. Vis. Graphics Image Process.* **23**, 341–352. [https://doi.org/10.1016/0734-189X\(83\)90032-4](https://doi.org/10.1016/0734-189X(83)90032-4) (1983). <https://doi.org/>
48. Mayerhoefer, M. E. et al. Introduction to radiomics. *J. Nucl. Med.* **61**, 488–495. <https://doi.org/10.2967/jnumed.118.222893> (2020).
49. Benjamini, Y. & Hochberg, Y. Controlling the false discovery rate: A practical and powerful approach to multiple testing. *J. Royal Stat. Soc. Ser. B (Methodological)*. **57**, 289–300 (1995).
50. Jansson, L. M. & Patrick, S. W. Neonatal abstinence syndrome. *Pediatr. Clin. North. Am.* **66**, 353–367. <https://doi.org/10.1016/j.pcl.2018.12.006> (2019).
51. West, K. D., Ali, M. M., Blanco, M., Natzke, B. & Nguyen, L. Prenatal substance exposure and neonatal abstinence syndrome: state estimates from the 2016–2020 transformed medicaid statistical information system. *Matern Child. Health J.* **27**, 14–22. <https://doi.org/10.1007/s10995-023-03670-z> (2023).
52. Hirai, A. H., Ko, J. Y., Owens, P. L., Stocks, C. & Patrick, S. W. Neonatal abstinence syndrome and maternal Opioid-Related diagnoses in the US, 2010–2017. *JAMA* **325**, 146–155. <https://doi.org/10.1001/jama.2020.24991> (2021).
53. Balalian, A. A. et al. Prenatal exposure to opioids and neurodevelopment in infancy and childhood: A systematic review. *Front. Pediatr.* **11**, 1071889. <https://doi.org/10.3389/fped.2023.1071889> (2023).

Acknowledgements

The authors would like to acknowledge Sundar Paramasivam for his help with IT management.

Author contributions

JC contributed to the assessment and manuscript preparation, RV contributed to the design, analysis, and manuscript preparation, DH contributed to subject recruitment and manuscript review, IH contributed to study

procedures and manuscript review, SS contributed to subject recruitment, manuscript review, and funding, and RR contributed to conception, design, analysis, subject recruitment, manuscript preparation, and funding.

Funding

This work was supported by the following grants through the National Institutes of Health: R01DA059321 – MPI Radhakrishnan and Sadhasivam, R01HD096800 – PI Sadhasivam, and R03DA305679 – PI Radhakrishnan.

Declarations

Competing interests

Dr. Sadhasivam received pay from UpToDate: Anesthesia for Tonsillectomy and Neuroptics, Inc for studying opioid-induced respiratory depression in pediatric tonsillectomy. Dr. Sadhasivam is one of the inventors in the approved U.S. patents focused on opioid pharmacogenetics: U.S. Patent No. 9944985, 10662476, 16/850537, 16/946401, 16/946399, 10878939 and has not received any royalty so far. Dr. Sadhasivam is the founder and chief medical officer of OpalGenix, Inc with equity interest. Dr. Sadhasivam is the chief medical officer of NCAP Medical, LLC with equity interest. There is no financial conflict with the current article.

Additional information

Supplementary Information The online version contains supplementary material available at <https://doi.org/10.1038/s41598-025-27486-9>.

Correspondence and requests for materials should be addressed to R.R.

Reprints and permissions information is available at www.nature.com/reprints.

Publisher's note Springer Nature remains neutral with regard to jurisdictional claims in published maps and institutional affiliations.

Open Access This article is licensed under a Creative Commons Attribution-NonCommercial-NoDerivatives 4.0 International License, which permits any non-commercial use, sharing, distribution and reproduction in any medium or format, as long as you give appropriate credit to the original author(s) and the source, provide a link to the Creative Commons licence, and indicate if you modified the licensed material. You do not have permission under this licence to share adapted material derived from this article or parts of it. The images or other third party material in this article are included in the article's Creative Commons licence, unless indicated otherwise in a credit line to the material. If material is not included in the article's Creative Commons licence and your intended use is not permitted by statutory regulation or exceeds the permitted use, you will need to obtain permission directly from the copyright holder. To view a copy of this licence, visit <http://creativecommons.org/licenses/by-nc-nd/4.0/>.

© The Author(s) 2025